11

Construction of a Vertical Displacement Service Robot with Vacuum Cups

Nicolae Alexandrescu[1], Tudor Cătălin Apostolescu[2], Despina Duminică[1], Constantin Udrea[1], Georgeta Ionaşcu[1] and Lucian Bogatu[1]
[1]*"POLITEHNICA" University of Bucharest*
[2]*"TITU MAIORESCU" University of Bucharest*
Romania

1. Introduction

Based on the results of interdisciplinary fields like mechanics, electronics and informatics the autonomous mobile robots are gaining more and more attention. The methods used for movement, actuation and none the last the ability to operate in unknown and dynamic environments give them a great complexity and a certain level of intelligence.
The human model is still a challenge for mobility and robot movement. Robot mobility is satisfactorily achieved, in some cases even better with other types of locomotion means, but technical solutions that rigorously reproduce human walking are not yet identified.
Feasible solutions can be found in the situation when human mobility reaches its limits (movement on planes with high inclination angles, including 90° – vertical and 180° – parallel to the horizontal plane – ceiling type). Autonomous robot mobility on planes characterized by high inclinations is less tackled in specialty literature, some encountered solutions being objects of patents. The research in this field has a tremendous potential especially in providing new ideas and/or knowledge development.
The field of professional and domestic services, especially the wall cleaning of high buildings, is one of the areas that are expected to obtain a strong benefit from the use of robotic systems able to displace on vertical surfaces.
The advantages of the technologies that use climbing and walking robots consist mainly of two aspects:

- automatic cleaning of high buildings, improvement of technological level and of productivity of service industry in the field of building maintenance;
- cleaning robots can be used on various types of building, avoiding thus high costs involved by permanent gondola-type systems (open platform-car or baskets) for individual buildings.

The most common attachment principle is the vacuum adhesion (Cepolina et al., 2003), (Miyake et al., 2007), (Novotny&Horak, 2009), where the robot carries an onboard pump to create a vacuum inside the cups, which are pressed against the wall. This system enables the robots to adhere on any type of material, with low energy consumption. Vacuum adhesion is suitable for usage on smooth surfaces, because the roughness can influence a leakage loss in the vacuum chamber.

The mobile robots endowed with platforms and legs with cups are widely spread in practical applications due to high relative forces of locomotion, mobility and good suspension. The disadvantage of increased overall size less disturbs in applications of cleaning and inspection of large vitrified surfaces covering the buildings, (Sun.et al., 2007).
A new generation of cleaning robots based on all-pneumatic technology is on study (Belforte et al., 2005).
In this context, the authors developed an original solution of a cleaning robot with vertical displacement and vacuum attachment system (Alexandrescu, 2010a, 2010b), (Apostolescu, 2010). The novelty of the approach consists of the robot capability to move on vertical surfaces, which involves basic studies enlarging the horizon of knowledge related to: displacement cinematic structures, robot leg anchoring solutions, actuating solutions, as well as control system of such robots.

2. Robot construction

The robot structure (Fig. 1) contains two triangular platforms with relative mobility and reduced overall size. It is an original feature, not being found till now in the structure of the robots moving in the vertical plane. The fixing of the robot on the vertical surface is achieved by vacuum cups.

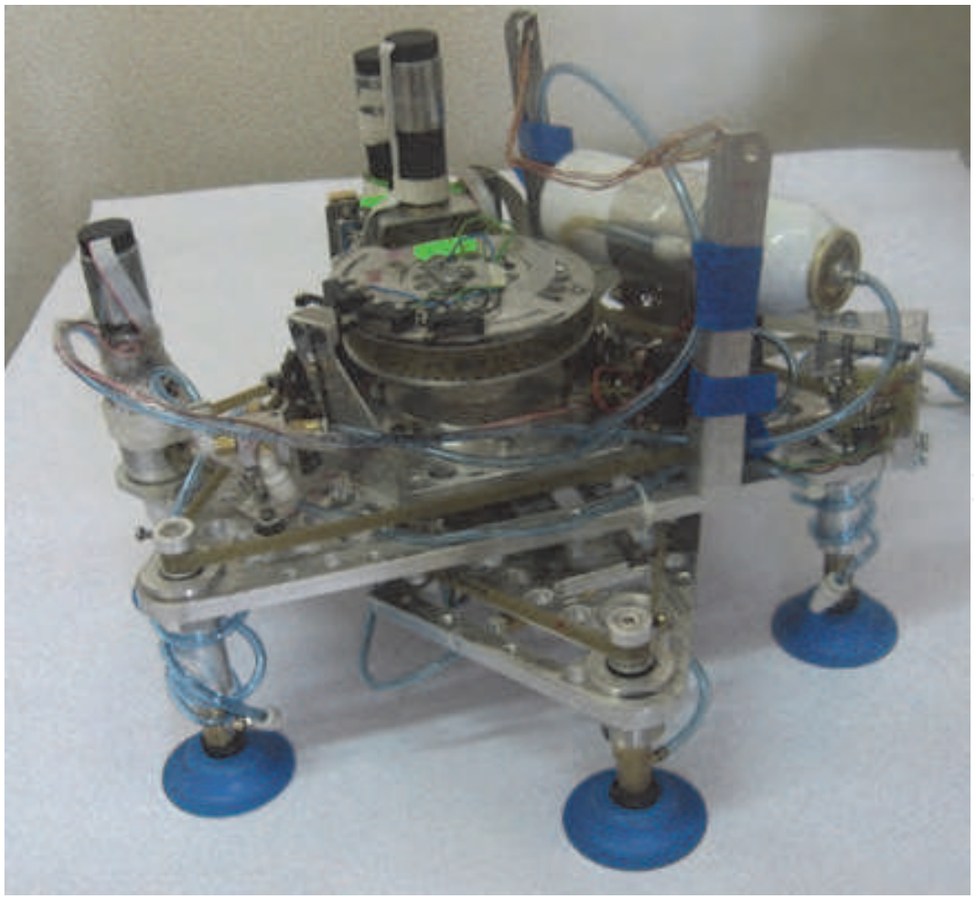

Fig. 1. The autonomous robot with vertical displacement

In order to obtain an autonomous robot, the electric actuation of all degrees of freedom was chosen, as well as for the depressurization needed by the cups. An original driving system was introduced for the moving of robot legs. The system uses screw mechanisms synchronized by a toothed belt transmission. The system developed for the relative translation of the platforms contains a ball guideway of reduced size and good guiding accuracy. The use of a rack mechanism allows a compact and fast actuation. The rotation of the robot is achieved by modifying the relative angular position of the two platforms.
The kinematic scheme of the robot is presented in Fig. 2. Although the robot attaches itself to the glass surface by the means of vacuum cups, a significant miniaturization was achieved.
The interior platform – PLE - 7 is fixed on three vacuum suction cups 9. The raising and lowering of the platform is controlled using a screw mechanism 8 actuated by the motor-reduction gear M_1R_1. The toothed driving belt 4 allows the synchronous movement of the three suction cups. Similarly, for the exterior platform – PLE - 3 we have suction cups 1, the mechanism 2 and the motor-reduction gear M_2R_2 .

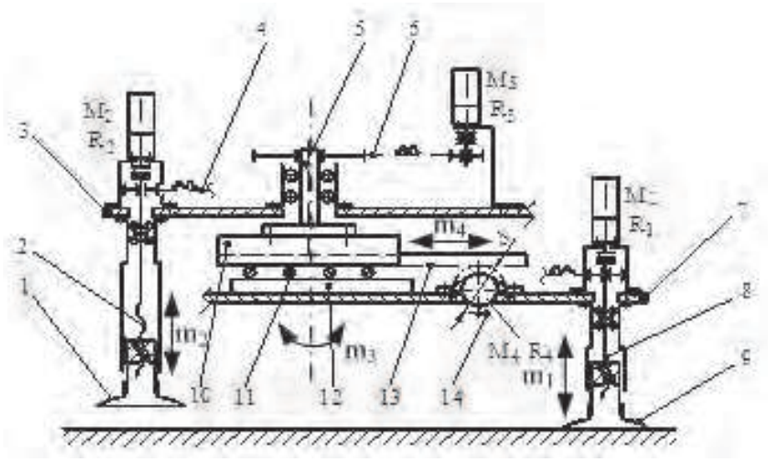

Fig. 2. The kinematic scheme

The driving toothed belt 6 and the motor-reduction gear M_3R_3 – movement m_3 allow the orienting rotation of the robot. The guiding part 10 is fixed on the shaft 5.
Translation between platforms – movement m_4 is achieved by the means of motor-reduction gear M_4R_4 fixed on the interior platform 7. A mechanism consisting of the gear 14 and the rack 13 solidary with the guiding part is used. This type of mechanism was preferred instead of a screw mechanism which would be difficult to miniaturize. A rolling guideway 11 is also used.
Figure 3 presents the 3D model of the robot placed in two positions: on a horizontal surface (Fig. 3a) and on a vertical surface (Fig. 3b).
The main parameters of the robot are:

- triangular platform side length L = 247 mm, corresponding to a stroke S of about 100…110 mm;
- full cycle for a translation step: 200…220 mm;
- duration of a cycle: 8s;
- vacuum of Δp=0.57 bar;
- diameter of the vacuum cups: 50 mm;
- normal detachment force: 86 N;
- lateral detachment force: 110 N;
- cup raising and lowering speed: approx. 6mm/s.

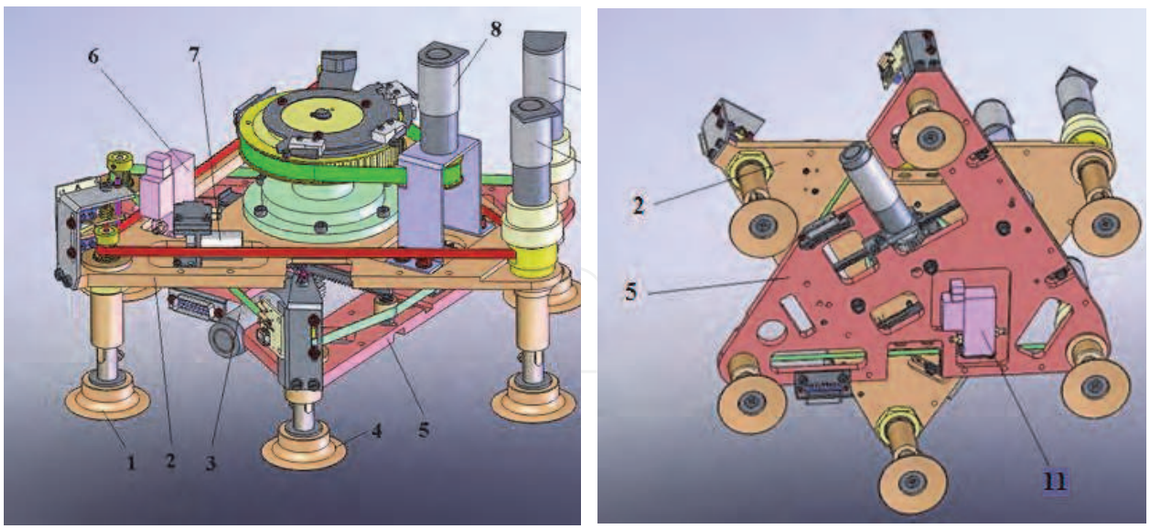

a) b)

Fig. 3. The 3D model of the robot: a) on a horizontal surface; b) on a vertical surface

The pneumatic diagram used for reducing the pressure inside the cups of the robot legs, in order to ensure the contact force when vacuumed suction cups adhere on the surface to be cleaned, is presented in Fig. 4: PV - vacuum micro pump (NMP 015 B – KNF Neuberger); Ac - tank; EM1, EM2 - electromagnets for the electro valve operating; V1, V2, V3 - vacuum cups for the interior platform; V4, V5, V6 - vacuum cups for the exterior platform; D - depressurization; A - atmospheric pressure.

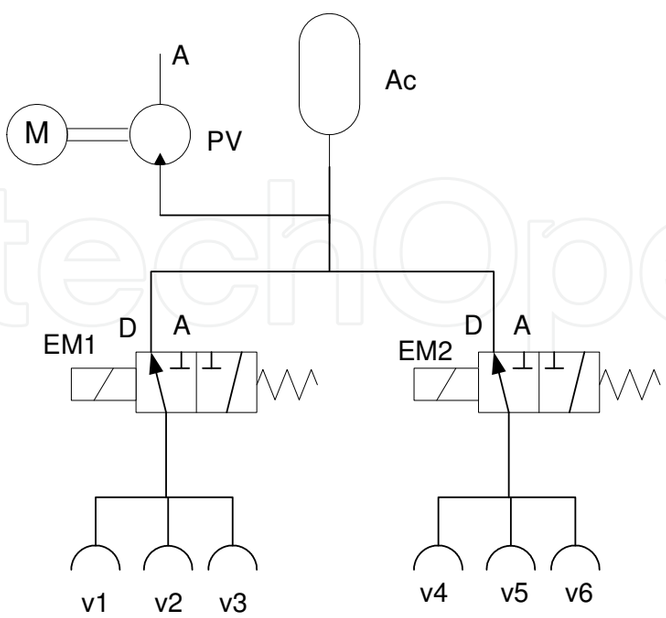

Fig. 4. Pneumatic diagram

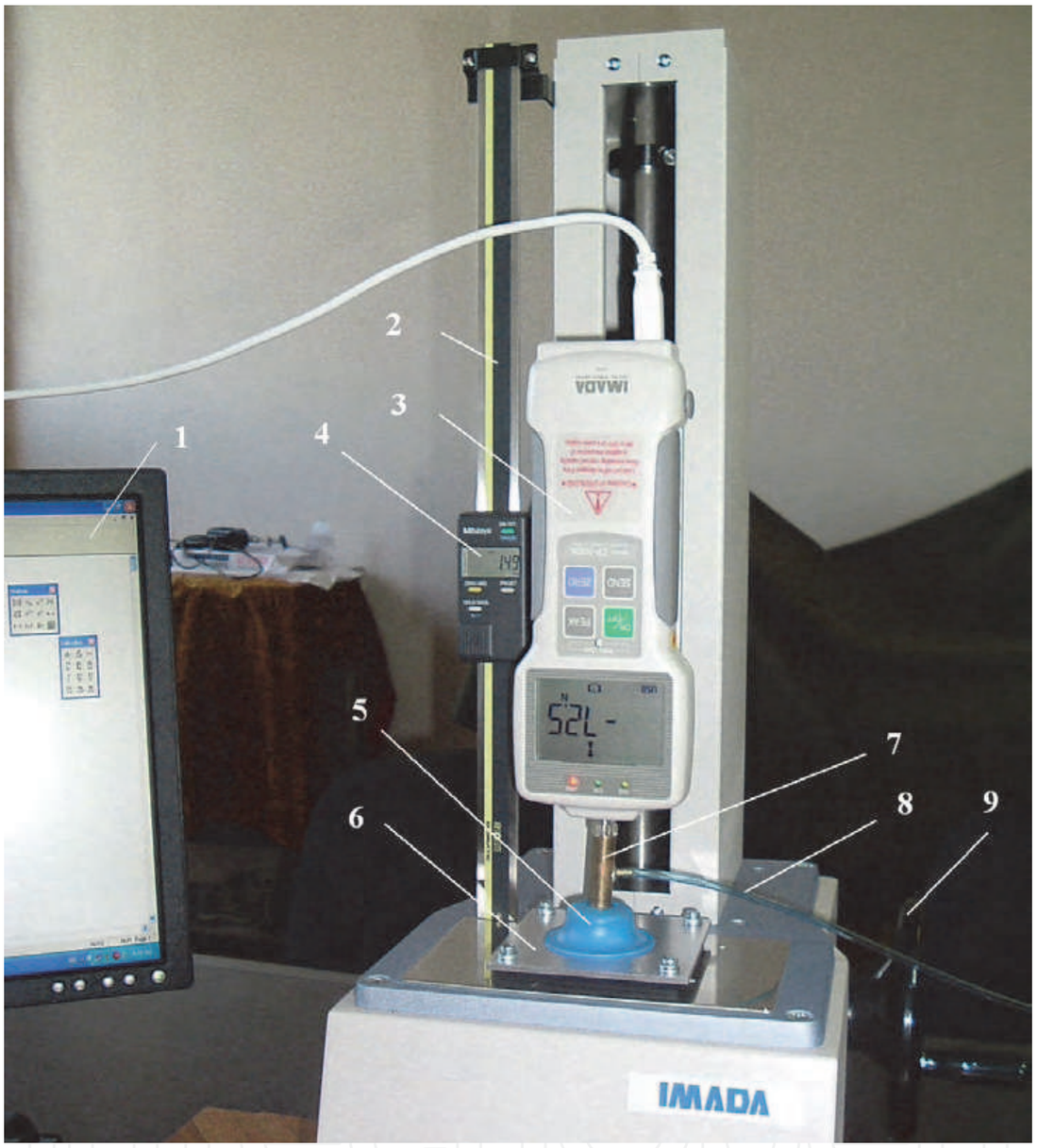

Fig. 5. Test stand used in order to establish the cup characteristic in the presence of normal forces F_x: 1 - computer, 2 - incremental rule, 3 - dynamometer, 4 - electronic vernier, 5 - vacuum cup, 6 - working surface, 7 - rod, 8 - table, 9 - hand wheel for obtaining the displacement w_x.

3. Research of the vacuum attachment system of the robot

An important part of the research concerned the fixing of the robot on the vacuum cups (Alexandrescu, 2010b). In order to establish their bearing capacity, the cups were subjected to external normal, lateral and combined loads. Tests were performed for different depressions. The influence of the different supporting materials was also studied, as well as the behaviour of the cup in presence of different liquids on the surface.

ESS-50 vacuum cups (FESTO) with an outer diameter of 50 mm were used. Glass (R_a=0.02µm), polished aluminium (R_a=0.59µm;) and textolite (R_a=1.1µm) were used as supporting surface. Different functional conditions were simulated. The roughness was measured using the roughness tester Surftest SJ 201P (Mitutoyo). Different working conditions were generated: cleaning of dry surfaces, cleaning of watered surfaces and cleaning using window detergent solution.

Fig. 5 presents the experimental stand used for the study of the effects of normal forces F_x.

Figure 6 presents the results obtained for dry glass surfaces. The positive values of the force correspond to the tendency of wrenching/detachment of the cup. The negative values of the force are conventionally assigned to the compression tendency of the cup.

Tests were performed also on dry aluminium surfaces and on dry textolite surfaces. The obtained diagrams are similar. Only small differences are noticed among the values corresponding to the three materials. For reduced deformations, glass and textolite have almost the same behaviour.

In fact, values of the roughness below 1µm do not influence the detachment force. Only the aluminium surface requires smaller loads.

In the range of negative deformations (cup compression), rigidity of the elastic membrane is the only factor that influences the characteristic, thus the three diagrams are very similar.

The study performed on watered surfaces showed almost insignificant decrease of the cup performance, due to the fact that water was practically eliminated from the contact area during cup fixing.

A most significant reduction of maximum normal load was noticed when detergent for window cleaning was used, because it remained in the contact area even after the cup was fixed on the supporting surface.

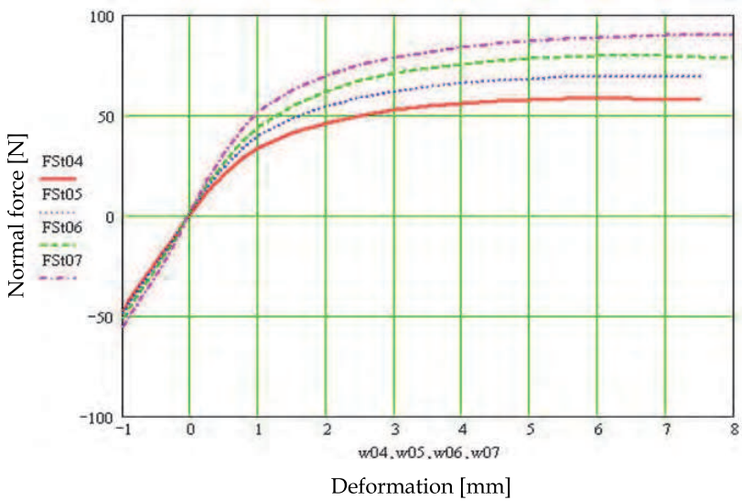

Fig. 6. Experimental diagrams obtained for dry glass, normal force; FSt04 – depression of 0.4bar; FSt05 – depression of 0.5bar; FSt06 – depression of 0.6bar; FSt07 – depression of 0.7bar.

Figure 7 presents the diagrams obtained for glass surfaces in the three situations. A decrease of about 6% of the cup capacity appears in the presence of detergent.

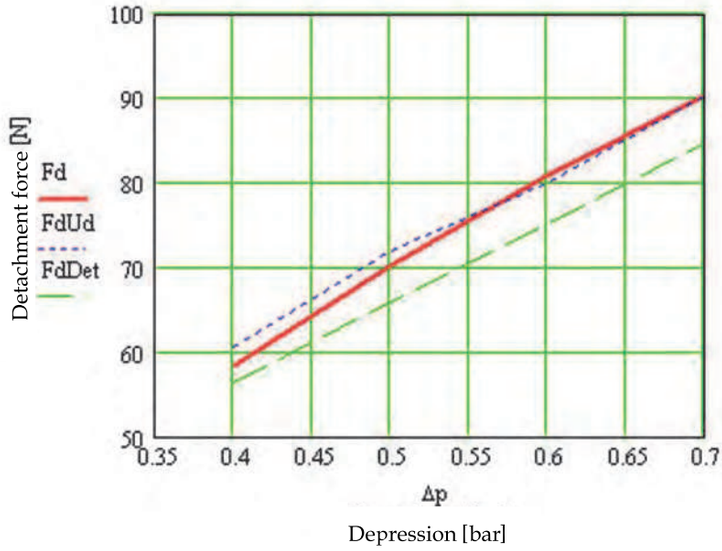

Fig. 7. Comparation among the maximum values of the detachment force: Fd – dry glass; FdUd – watered glass; FdDet – glass with detergent for window cleaning.

The test stand presented in Figure 8 was developed for the study of cup fixing on vertical planes.
In the presence of lateral forces, it was noticed that a slip of the cup appeared, leading to the re-positioning of the cup on the supporting surface. The slip stopped and the cup stabilized itself after 5…10s.
In order to deliver a correct information regarding the characteristic of the cup, after its stabilization, the deformation presented on the diagrams is obtained as difference between the total deformation obtained by progressive loading and the lateral slips.
The obtained results are presented in Figure 9. It can be noticed that the maximum supported loads are 50%-76% larger in the case of lateral forces that in the case of normal forces, an important advantage for a vertical robot. Similar results were obtained in the cases of aluminium and textolite.
Figure 10 presents a comparison among the three working surfaces for a depression of Δp=0.7bar. It can be noticed that the behaviour of the cup is practically identical.
The last part of the experimental research concerned the study of the cup behavior in presence of combined forces. The tests were performed for a maximum value of the normal force of F_n=49N, generated by the compression f=9mm of the spring 17 (Fig. 8). This force corresponds to approximately 60% of the normal detachment force previously established.
The diagrams corresponding to the tests on dry glass, in the presence of combined forces, are shown in Figure 11.
The same values of the depression as in the previous experiments were used for tests.
A comparison between the behaviour of the cup subjected to combined forces and subjected only to a normal force is presented in Figure 12. Experiments showed that, when lateral and normal forces acted together, the values of lateral forces were 36…45% smaller than in the absence of normal forces. Tests performed on aluminium and textolite surfaces led to similar results.
As previously, the research covered also the situation of fixing on watered glass. In the presence of lateral forces, the values of the cup slip increased significantly, e.g. for a depression of 0.6bar the slip exceeded 2mm. The obtained diagram is presented in Figure 13.

If the cup was supported on glass surfaces washed with detergent for window cleaning, the values of maximum lateral forces decreased with another 10…15%.
The experimental results obtained for aluminium and textolite were comparable to the results obtained in the case of glass supporting surfaces.

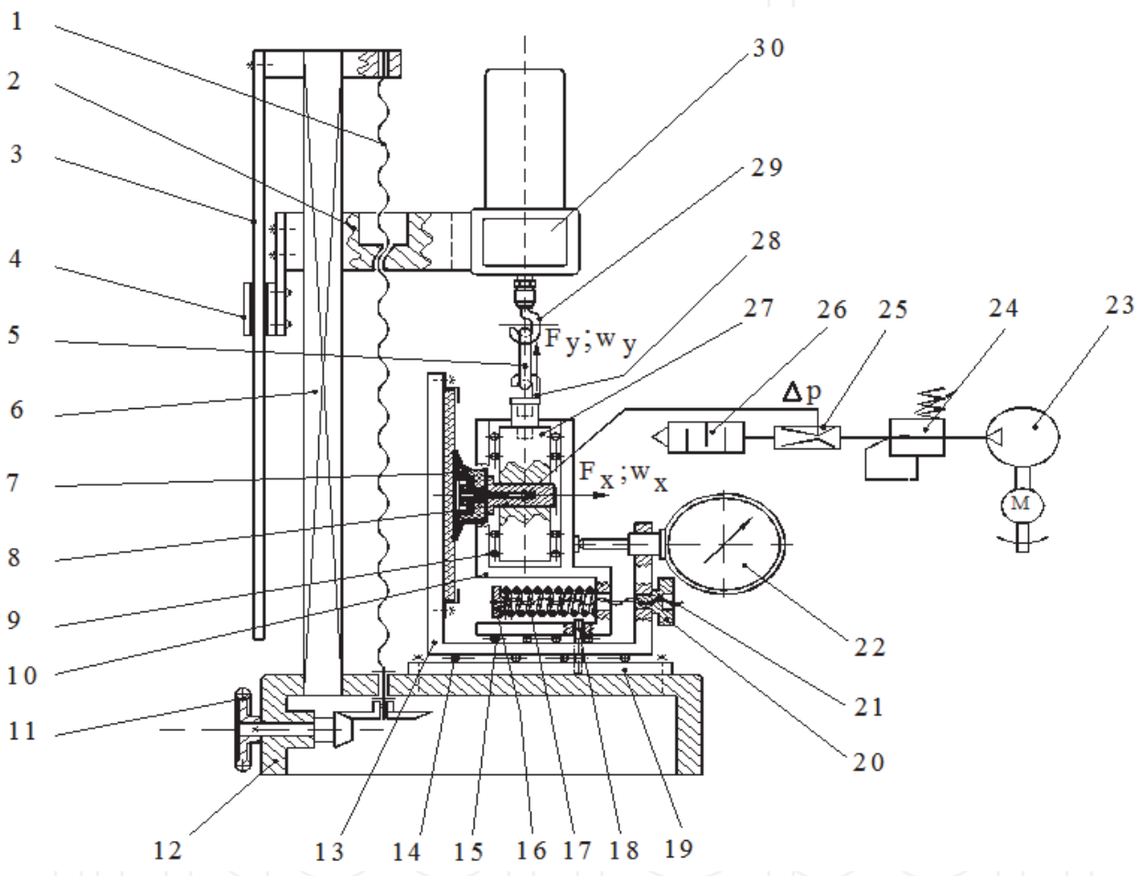

Fig. 8. Scheme of the experimental stand developed for testing the cups subjected to lateral forces F_y: 1 – screw for the displacement w_y; 2 –guide yoke; 3 –Vernier rod; 4 – digital vernier for w_y; 5 – link for transmitting the force F_y; 6 – guiding riser; 7 – cup; 8 – cup fixing body; 9, 14, 15 – ball guides; 10, 13, 27 – mobile elements; 11 – hand wheel w_y; 12 – dynamometer body; 16 – pan; 17 –spring for generating the force F_x; 18 – rod for positioning the element II; 19 – base; 20 - hand wheel w_x; 21 - screw for generating the force F_x; 22 – dial gauge; 23 – compressor; 24 – pressure regulation; 25 – ejector; 26 – noise damper; 27 – element I; 28 – stand hook; 29 – dynamometer hook.

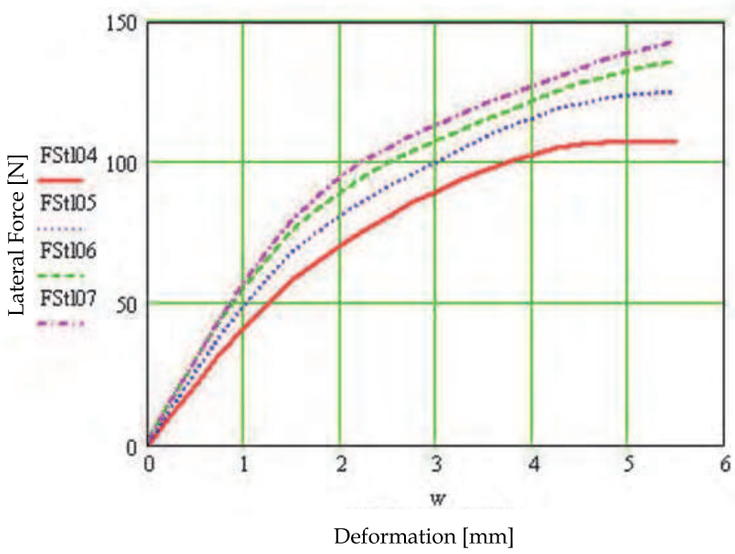

Fig. 9. Experimental diagrams for dry glass, lateral force; FSt04 – depression of 0.4bar; FSt05 – depression of 0.5bar; FSt06 – depression of 0.6bar; FSt07 – depression of 0.7bar.

Due to the fact that design conditions imposed a maximum robot leg slip of 0.5mm, the experimental research showed that the lateral forces corresponding to the vertical fixing of the robot must not exceed 25…30N. The values of the allowed lateral forces were 50…60% smaller than in the case of fixing on dry glass.
The results contributed significantly to the development of a robot able to sustain its own weight on vertical surfaces in order to perform cleaning tasks.

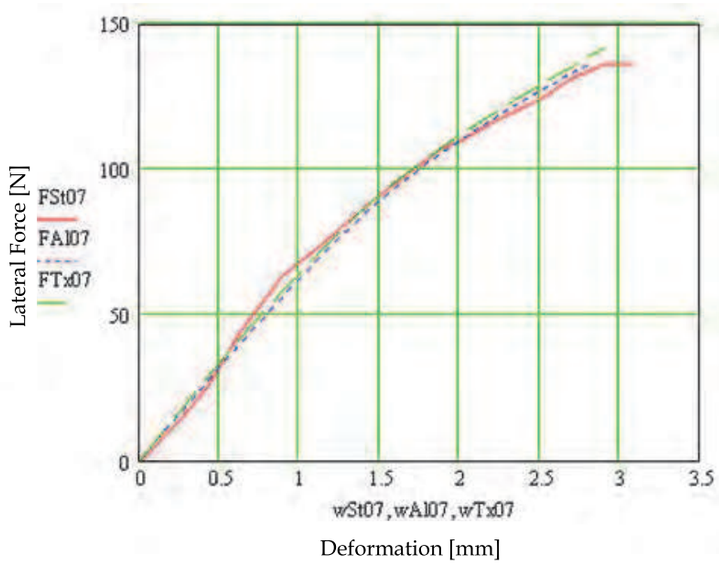

Fig. 10. Cup behavior in the presence of lateral force; depression of 0.7bar, different working surfaces: FSt07 – glass; FAl07 – aluminium; FTx07 – textolite.

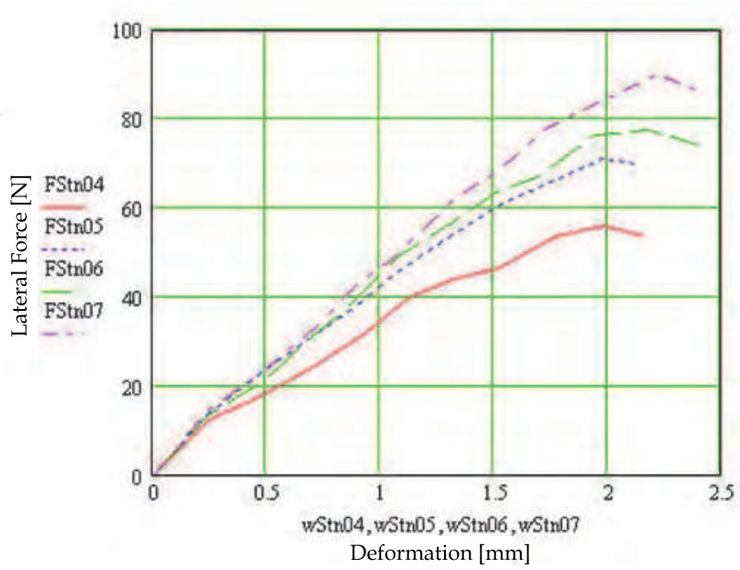

Fig. 11. Results of tests performed for combined forces (lateral force and normal force of 49N), for dry glass; FStn04 – depression of 0.4bar; FStn05 – depression of 0.5bar; FStn06 – depression of 0.6bar; FStn07 – depression of 0.7bar.

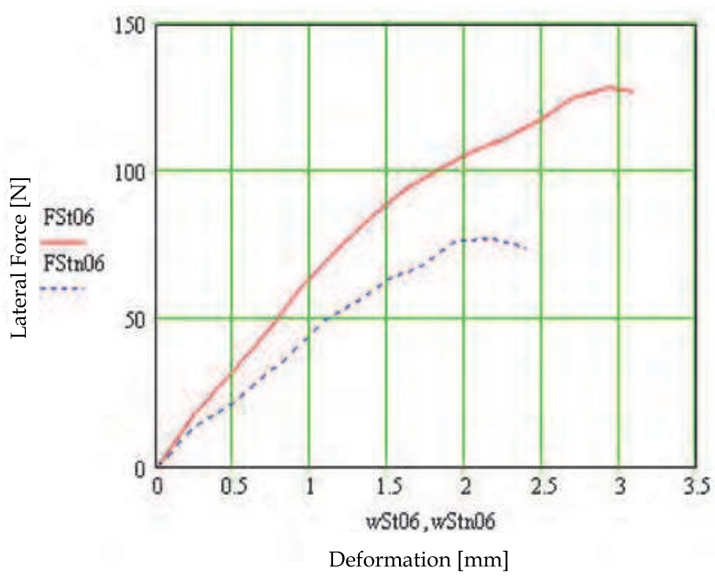

Fig. 12. Comparison between the behavior of the cup subjected to combined forces (FStn06) and normal force (FSt06) for a depression of 0.6 bar

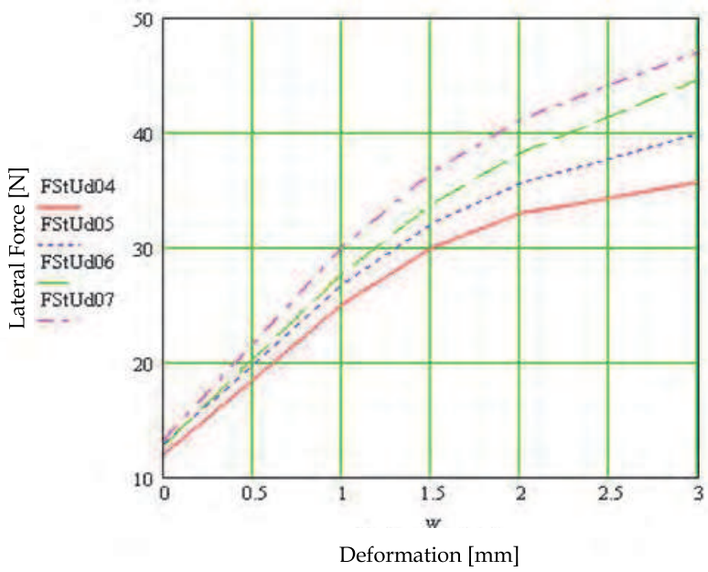

Fig. 13. Experimental diagrams for watered glass, lateral force; FStUd04 – depression of 0.4bar; FStUd05 – depression of 0.5bar; FStUd06 – depression of 0.6bar; FStUd07 – depression of 0.7bar.

4. Displacement kinematics

The value of the triangular platform side L = 247 mm was adopted in order to obtain a stroke S of about 100…110 mm. A translation of 200…220 mm of the robot is obtained for a full translation cycle (attachment on PLI suction cups – PLE translation - attachment on PLE suction cups - PLI translation), allowing the tracking of a glass surface of 1500 mm in about seven cycles. If a cycle duration of 8s is considered, the whole window size is travelled in less than one minute, which is convenient.

Figure 14 presents the constructive solution adopted for the robot displacement. The vacuum suction cup 1 (supplied from the vacuum miniature pump by the nozzle 16) is embedded in the sliding body 15 and can displace relatively to the guideway 3. The parallel key 2 restraints rotation.

The used mechanism consists of the shaft-screw 13 and the nut – interior thread manufactured in the body 15. The toothed belt 11 and the belt gear 6 solidary with the shaft allow the driving. Radial bearings 4 and stroke limiter with microswitch 7 can also be noticed.

The microswitches – two for each leg – are fixed on the corner brackets 8, adjustable relatively to the arm 5 solidary with the plate 12 (PLI). The positioning of the suction cup is discerned by the disk 10 driven by the rod 14 in contact with the inner part of the slider. The spring 9 helps maintaining this contact.

The displacements of the robot result as a combination of the following categories of movements: one-step translation, rotation and pseudo-circular movement (Alexandrescu, 2010a).

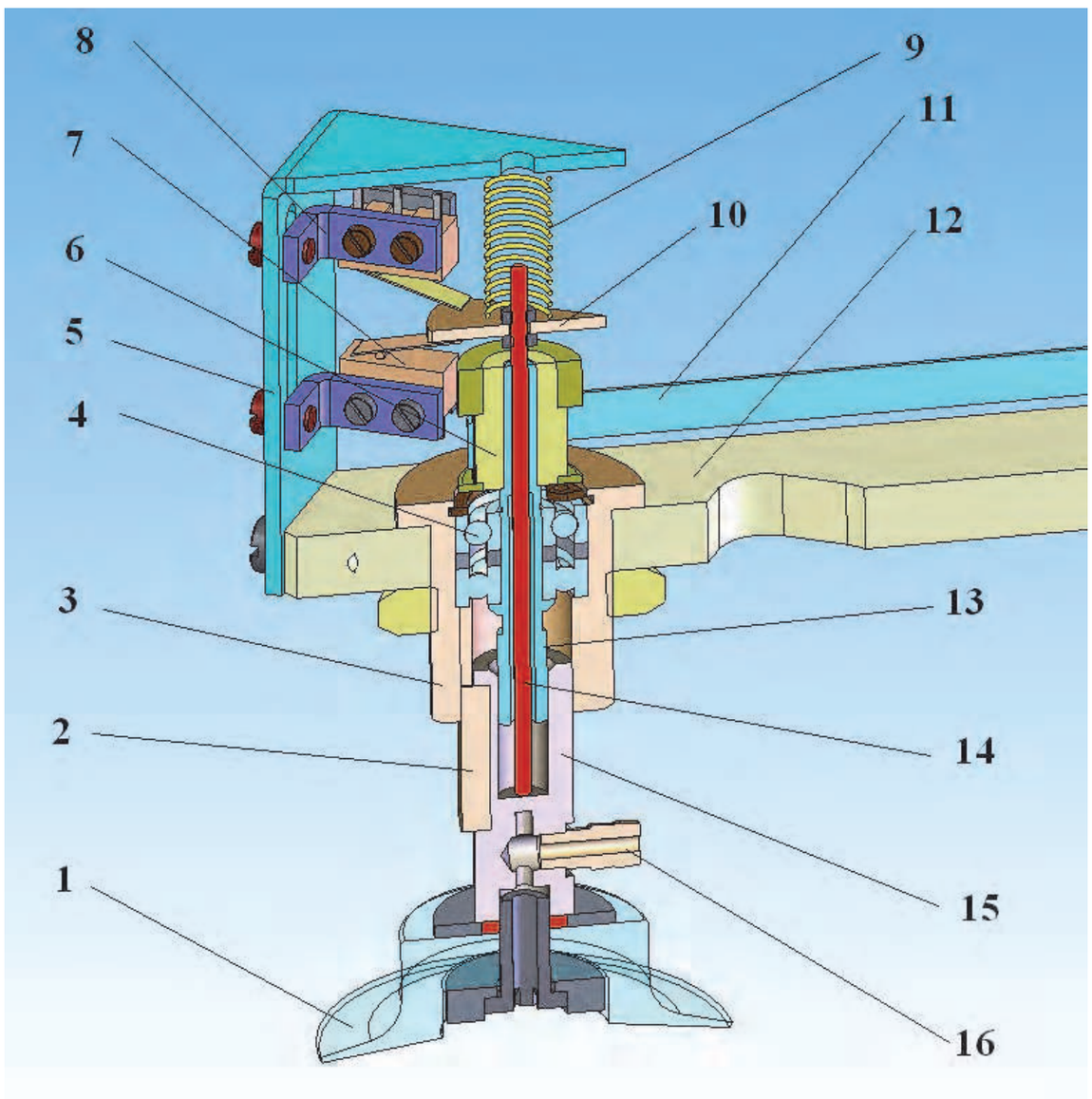

Fig. 14. Detail regarding the actuation of the displacement relative to the suction cups.

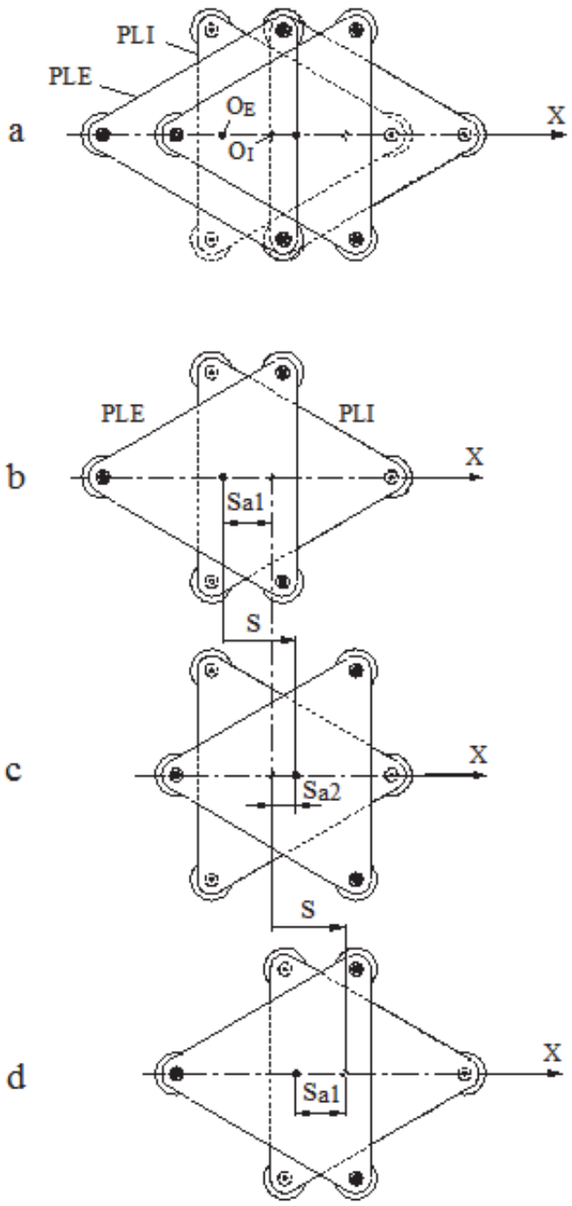

Fig. 15. One-step translation. a. Positions of the two platforms: PLE and PLI; b. Initial position; c. Position after PLE displacement; d. End position (after PLI displacement).

One-step translation of the robot involves the following sequence of movements, as shown in Figure 15. Notations from Figure 2 are used:

- PLE raising (movement $m_{2,up}$);
- PLE displacement (movement m_4);
- PLE lowering (movement $m_{2,down}$);
- PLI raising (movement $m_{1,up}$);
- PLI displacement (movement m_4);
- PLI lowering (movement $m_{1,down}$).

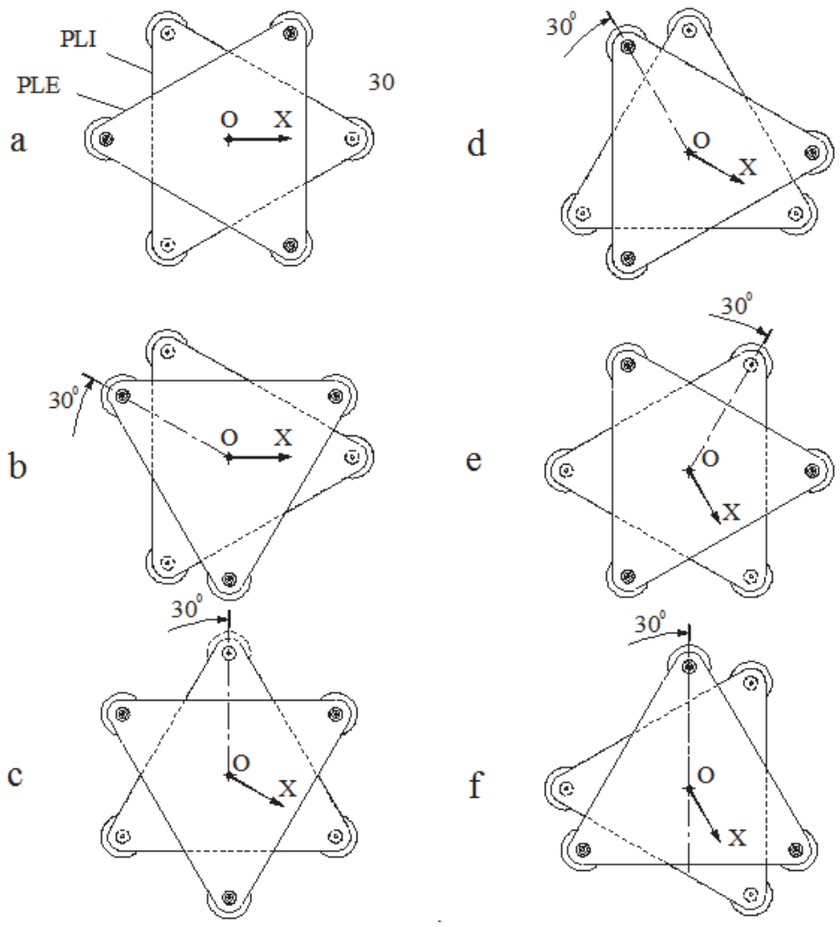

Fig. 16. Phases of a 90° clockwise rotation. a. initial state; b, d, f. Rotation FWD of PLE with 30°; c, e, g. Rotation RW of PLI with 30°.

Robot rotation is achieved by the following sequence of movements, as shown in Figure 16:

- PLE raising (movement $m_{2,up}$);
- PLE clockwise rotation of angle α (movement m_3);
- PLE lowering (movement $m_{2,down}$);
- PLI raising (movement $m_{1,up}$);
- PLI clockwise rotation of angle α (movement m_3);
- PLI lowering (movement $m_{1,down}$).

This sequence leads to a rotation of angle α = 30°, which is the recommended maximum angle of relative rotation between platforms. The sequence is repeated till the achievement of the desired angle rotation.

The counterclockwise rotation needs only reversing the direction of the partial rotations ($FWD \leftrightarrow RW$). Axis X indicates the direction of the sliding axis of the robot. Initial centring of platforms is needed.

The combination among a translation and a number of 30° rotations leads to a pseudo-circular movement outlining a 12-sided polygon, as presented in figure 17.

The translation has to start (point A of Figure 17,a) and to stop (point C of Figure 17,a) in a centred state (the centres of the platforms coincide).

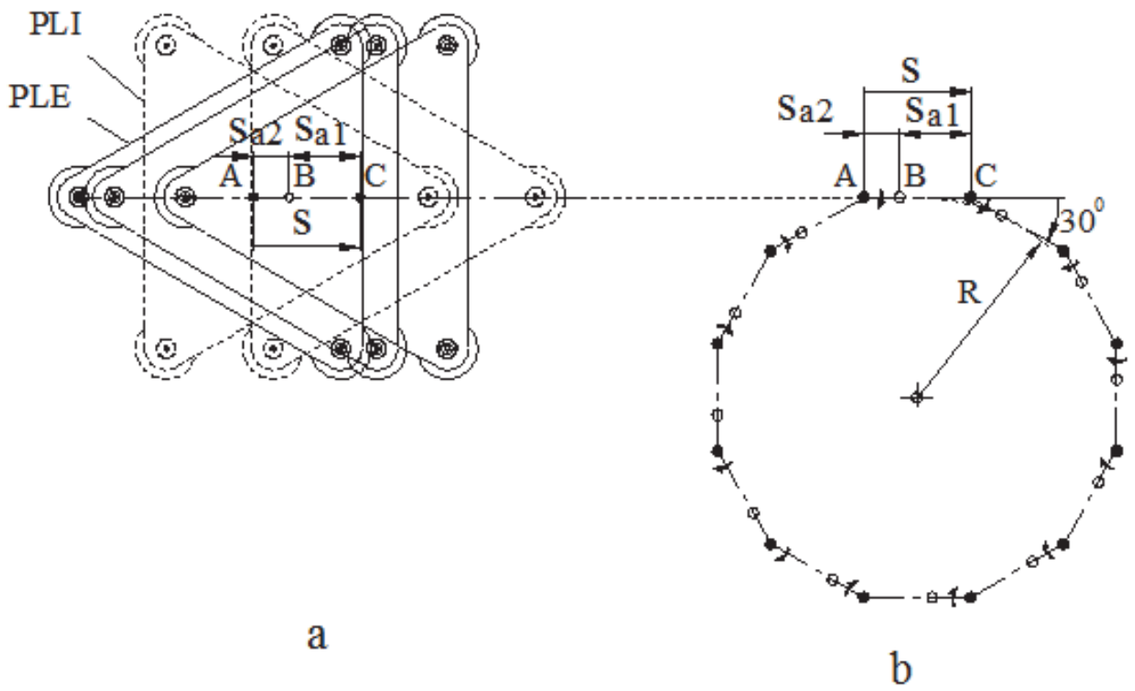

Fig. 17. Pseudo circular movement. a. the positions of the platforms PLE and PLI during translation; b. The polygon of the trajectory.

The radius of the circle inscribed in the travelled polygon is given by (1):

$$R = \frac{S}{2 \cdot tg15^{\circ}} \approx 1.867 \cdot S \tag{1}$$

5. Modelling and simulation of the robot displacement

The displacement of the robot was modelled and simulated using Cosmos Motion software (Alexandrescu, 2010a), (Apostolescu, 2010).

In order to simulate the robot translation, for the relative movement between platforms the interior platform was considered to be fixed. A parabolic variation was imposed for the acceleration. The numeric values used for simulation are: displacement $\Delta S = 100\ mm$, maximum acceleration a_{max} = 500 mm/s² and computed maximum speed v_{max} = 60 mm/s. Figures 18, 19 and 20 present the simulation results.

The simulations allowed the computation of the value of the maximum instantaneous power: P_{tr}= 0.69 W.

The needed power at the exit of the driving motor resulted equal to 1.42W.

The orienting rotation of the robot was simulated for rotation cycle of 30º. Figures 21, 22 and 23 present the simulation results.

In the transitory areas, it can be noticed that the variation of the angular acceleration presents deviations relatively to its theoretical shape. This phenomenon can be explained by the variation of the static charges during platform rotation.

The computed maximum value of the couple was equal to 0.204 Nm. The computed maximum power at the level of the platform was equal to Prot = 0.13 W.

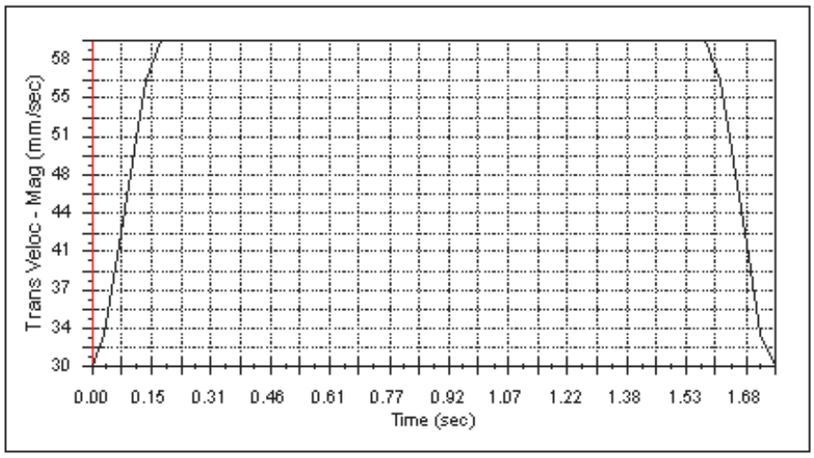

Fig. 18. Variation of translation speed.

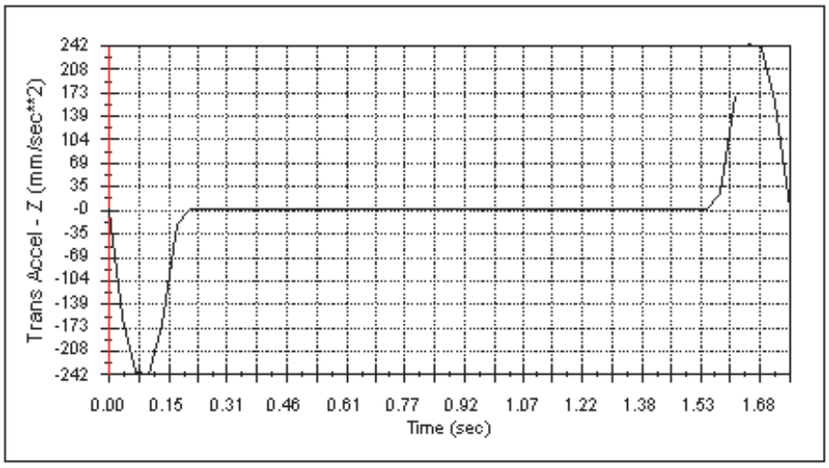

Fig. 19. Variation of translation acceleration.

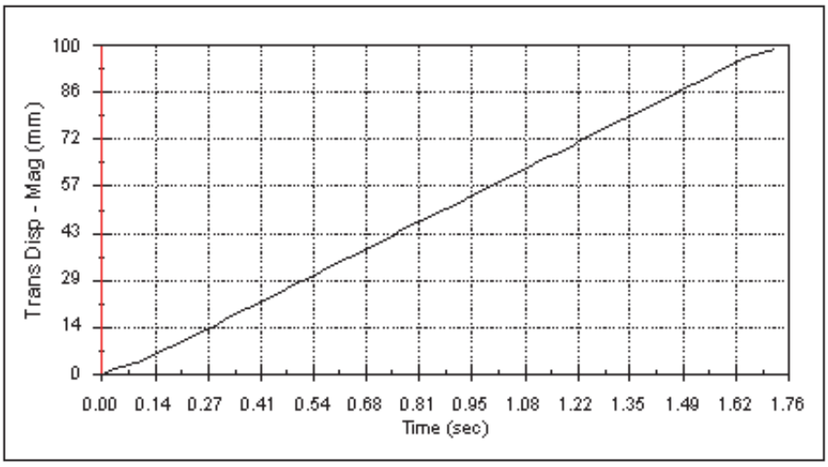

Fig. 20. Displacement during translation.

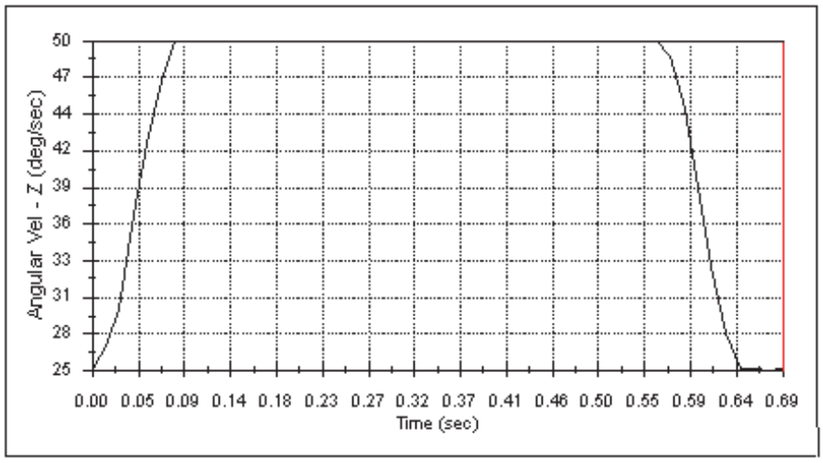

Fig. 21. Variation of angular speed during platform rotation.

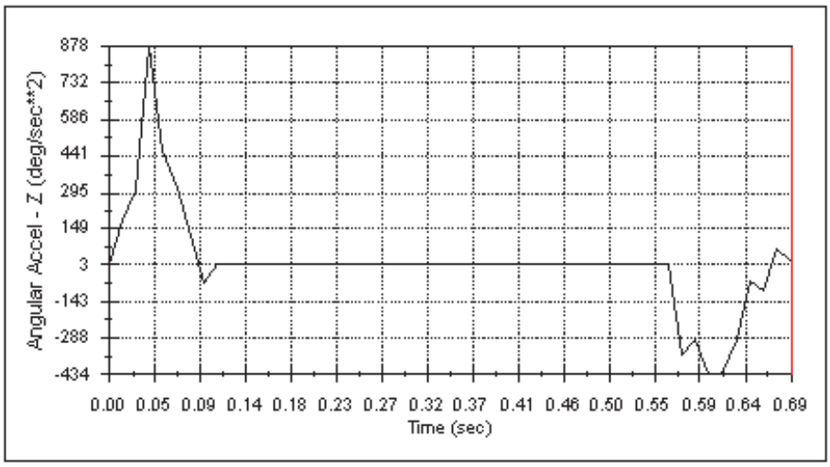

Fig. 22. Variation of angular acceleration during platform rotation.

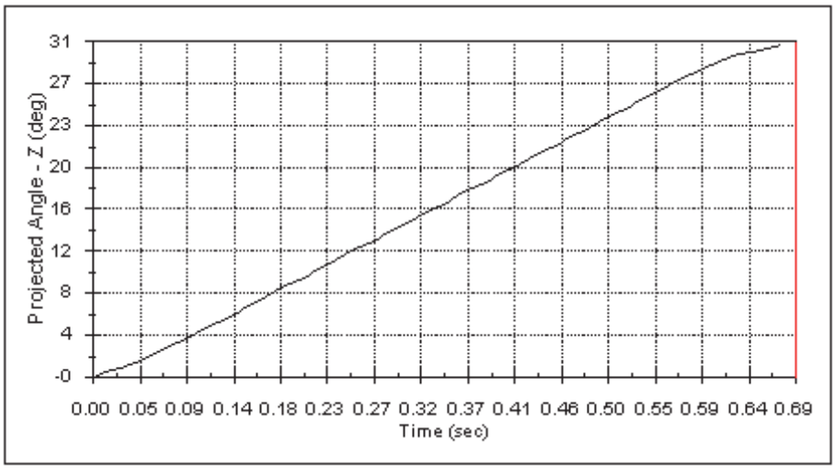

Fig. 23. Angle variation during rotation.

6. Robot control

The robot can be controlled with a data acquisition board 7344 National Instruments and LabVIEW programming or with microcontrollers. The microcontroller BS2 (Parallax) is used, easy to program but with a number of limitations concerning the control of motor speeds.

Using a data acquisition board allows introducing home switches for each of four servo axes in order to find the reference position. For axis 1 (robot translation) and axis 4 (orienting rotation), home switches are mounted between the limiting micro switches. For axes 2 and 3, representing cup translations for PLE and PLI, respectively, micro switches are used only as stroke limit. The reference position is found with the help of a photoelectric system, as shown in Figure 24. The system consists of a light stop 6 fixed on the mobile plate 4 whose displacement *s* gives the position of the cups. The light stop moves between the sides of the photoelectric sensor 2 (of type OPB 916).

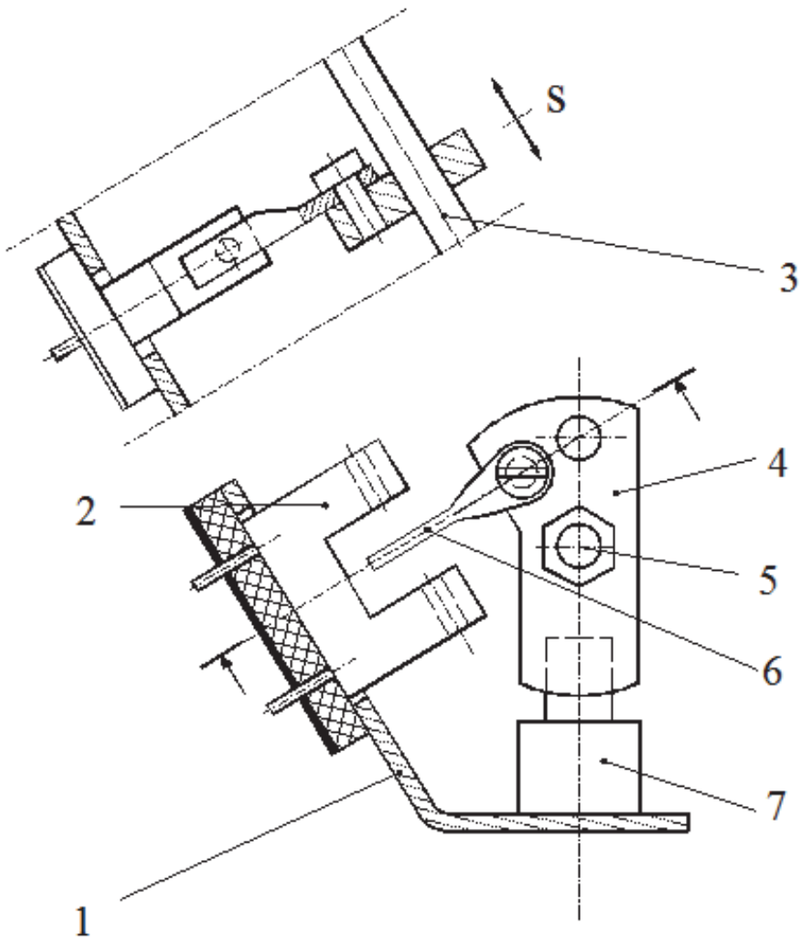

Fig. 24. Photoelectric system used in order to establish the reference position of axes 2 and 3. 1 – corner support; 2 – photoelectric sensor; 3 – rod for movement obstruction; 4 – plate attached to the mobile rod; 5 – mobile rod; 6 – light stop; 8 – microswitch.

Figure 25 presents the scheme of the photoelectric system used to determine the reference position. When the light stop reaches the optical axis of the sensor, the state of its output changes. The emitter diode is supplied through the resistor R_a for current limitation. A power amplifier OPB916 is connected at the circuit output. The suppressor diode D_s protects the transistor during its disconnection. Connection to the data acquisition board is made through the NO contact of the relay Rel.

The LabVIEW software program that allows founding the home switch is shown in Figure 26. The activation of limit switches is also needed during the search. After the reference is found, the position counter is reset. The program is applied for each of four axes of the acquisition board.

The programs consists of two sequences introduced by the cycle 10. The first one searches the reference position and the second resets the position counter (subVI 9).

The subVI 1 loads the maximum search speed and performs axis selection. The subVIs 2 and 3 load the maximum acceleration and deceleration. The subVI 4 defines the movement kinematics (S curve of the speed). A *while* type cycle is introduced. The subVI 7 reads the state of the search. The subVI 12 seizes various interruption cases. The subVI 13 stops the cycle.

In order to clean glass surfaces, the robot must cover the whole window area, paying especial attention to corners. The main control program of the robot controls the travel on the vitrified surface by horizontal and vertical movements, as well as by rotations that allow changing the direction. An ultrasonic PING sensor (Parallax) was introduced as decision element for changing the direction and stopping. The sensor is mounted on the PLI platform using the corner 3 and the jointed holder 2, as shown in Figure 27.

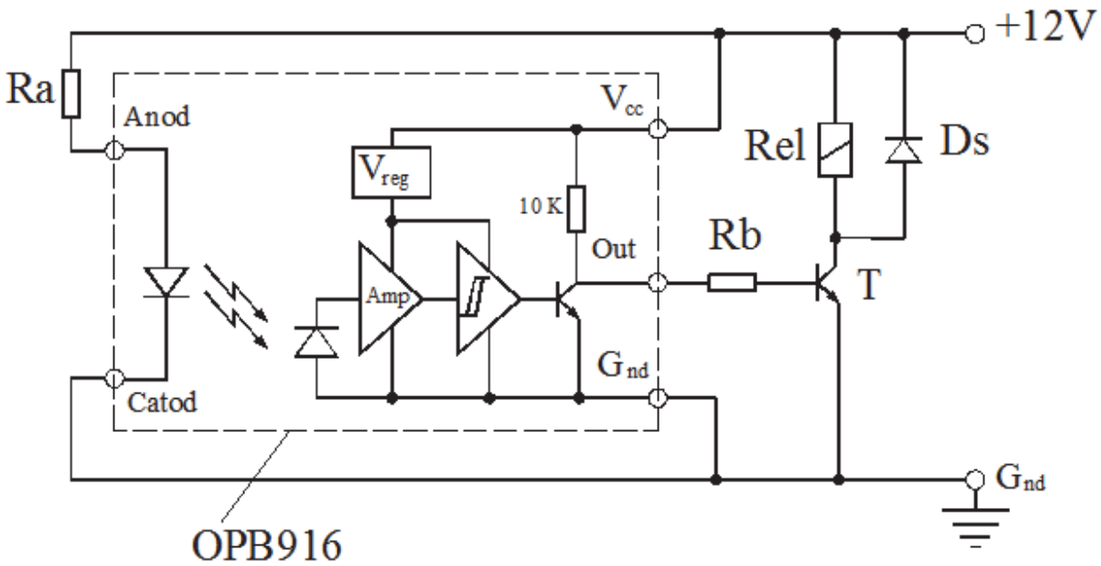

Fig. 25. Scheme of the photoelectric circuit.

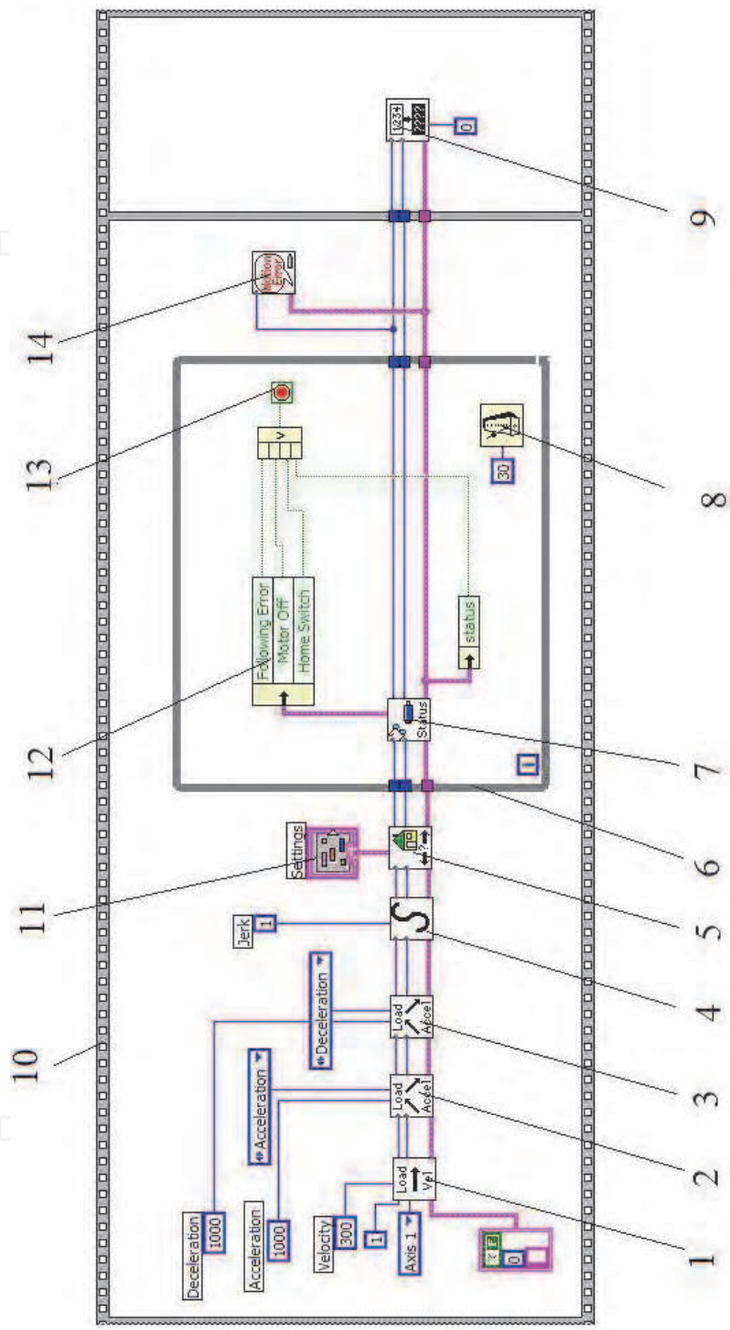

Fig. 26. LabVIEW program for founding the home switch: 1 – maximum speed load; 2 – acceleration load; 3 – deceleration load; 4 – elements of curve S (kinematics without jerk); 5 – home switch use; 6 –*while* type cycle; 7 – reading of search state; 8 – delay producing; 9 – position counter reset; 10 – sequential cycle with two sequences; 11 – search settings; 12 – reading of different interrupt situations; 13 –end cycle condition; possible errors indication of possible errors.

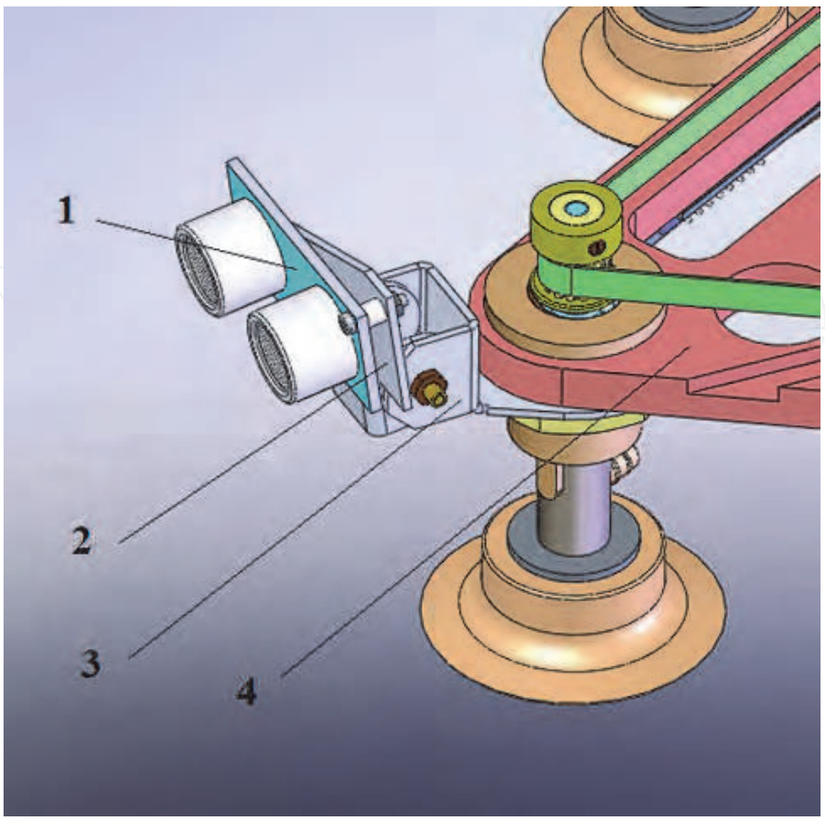

Fig. 27. The ultrasonic sensor mounted on the interior platform: 1 – sensor; 2 – sensor holder; 3 – corner; 4 – interior platform PLI of the robot.

Figure 28 presents a sequential cycle of travel. The cycle consists of the following sequences: sequential translation from left to right (this sequence ends when the proximity of the right side rim is sensed); 90° clockwise rotation; lowering with a step; 90° clockwise rotation; sequential translation from right to left (this sequence ends when the proximity of the left side rim is sensed); 90° counterclockwise rotation; lowering with a step; 90° counterclockwise rotation.

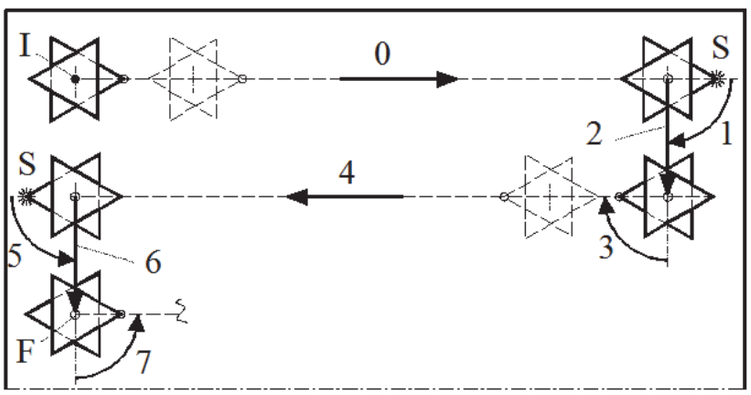

Fig. 28. Travel cycle of the robot.

The robot covers the whole window area by repeating the travel cycle. The robot stops if the sensor *S* sends the signal of proximity of the bottom rim of the vitrified surface.
The block diagram of the program is shown in Figure 29.

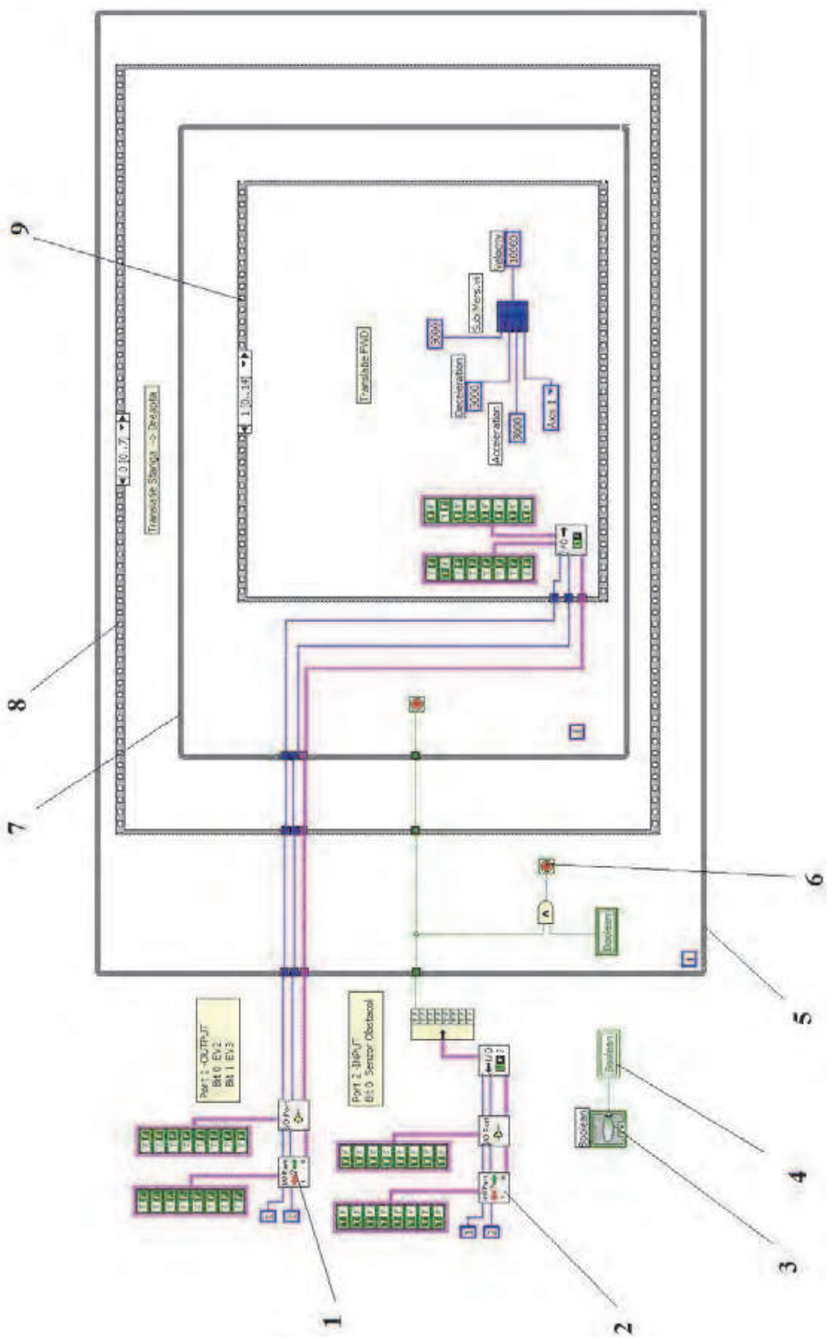

Fig. 29. Block diagram of main control program of the robot: 1 - setting port 1 as output; 2 - setting port 2 as input; 3 - initialization of local variable; 4 - boolean local variable; 5 – *while* cycle of the travel program; 6 – travel stop; 7 – first order *while* cycles; 8 – sequences of the first order cycles; 9 – sequences of the first order cycles.

The program uses the ports 1 and 2 of the acquisition board. The port 1 is used as program output, sending the commands towards the electro valves. The port 2 is used as input, receiving the signal from the sensor *S*. The control 3 initializes the boolean local variable as "False". The variable changes its state to "True" during vertical displacement. The signal from the sensor *S* is used also for stopping the horizontal translation sequences.

7. Conclusion

The chapter reports a number of very important results regarding the design and control of a prototype of climbing autonomous robot with vacuum attachment cups.
The robot construction is able to perform its intended function: the efficient cleaning of glass surfaces. The vacuum attachment system ensures good contact with the support surface, is simple and reliable. The modelling and simulation of the robot functioning, developed for platform translation as well as for relative rotation of the platforms, certifies that its performances are comparable to similar solutions conceived worldwide.
The overall size of the robot, 350mm x 350mm x 220mm, proves an optimal degree of robot miniaturization.

8. References

Alexandrescu, N.; Apostolescu, T.C.; Udrea, C.; Duminică, D.; Cartal, L.A. (2010). Autonomous mobile robots with displacements in a vertical plane and applications in cleaning services. *Proc. 2010 IEEE International Conference on Automation, Quality and Testing, Robotics*, Cluj-Napoca, Romania, 28-30 May 2010, Tome I, IEEE Catalog Number CFP10AQT-PRT, ISBN 978-1-4244-6722-8, pp. 265-270

Alexandrescu, N., Udrea, C., Duminică, D., & Apostolescu, T.C. (2010), Research of the Vacuum System of a Cleaning Robot with Vertical Displacement, *Proc. 2010 International Conference on Mechanical Engineering, Robotics and Aerospace ICMERA 2010*, Bucharest, Romania,2-4 December 2010, IEEE Catalog Number CFP1057L-ART, ISBN 978-1-4244-8867-4, pp. 279-283

Apostolescu, T.C. (2010) Autonomous robot with vertical displacement and vacuummetric attachment system (I Romanian), Ph.D. Thesis, POLITEHNICA University of Bucharest, 2010

Belforte G., Mattiazzo G., & Grassi R. (2005). Innovative solution for climbing and cleaning on smooth surfaces. *Proceedings of the 6th JFPS International Symposium on Fluid Power*, pp. 251-255,Tsukuba, Japan.

Cepolina, F.; Michelini, R.; Razzoli, R.; Zoppi, M. (2003). Gecko, a climbing robot for wall cleaning. *1 st Int. Workshop on Advances in service Robotics ASER03*, March 13-15, Bardolino, Italia, 2003, Available from http://www.dimec.unige.it/PMAR/

Miyake, T.; Ishihara, H.; Yoshimura, M. (2007). Basic studies on wet adhesion system for wall climbing robots. *Proc. 2007 IEEE/RSJ International Conference on Intelligent Robots and Systems*, San Diego, CA, USA, Oct.29-Nov.2, 2007, pp. 1920-1925

Novotny F.; Horak, M. (2009). Computer Modelling of Suction Cups Used for Window Cleaning Robot and Automatic Handling of Glass Sheets. In: *MM Science Journal*, June, 2009, pp. 113-116

Sun D., Zhu J., & Tso S. K. (2007), A climbing robot for cleaning glass surface with motion planning and visual sensing, In: *Climbing & walking robots: towards new applications*, pp.219-234, Hao Xiang Zhang (ed.), InTech, Retrieved from <http://www.intechopen.com/books/show/title/climbing_and_walking_robots_towards_new_applications>

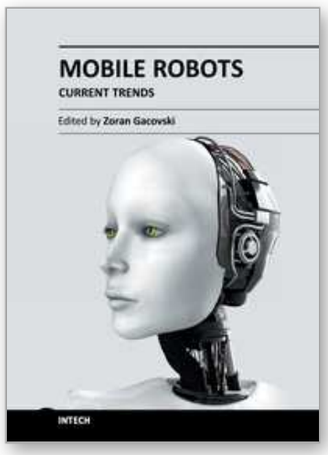

Mobile Robots - Current Trends

Edited by Dr. Zoran Gacovski

ISBN 978-953-307-716-1
Hard cover, 402 pages
Publisher InTech
Published online 26, October, 2011
Published in print edition October, 2011

This book consists of 18 chapters divided in four sections: Robots for Educational Purposes, Health-Care and Medical Robots, Hardware - State of the Art, and Localization and Navigation. In the first section, there are four chapters covering autonomous mobile robot Emmy III, KCLBOT - mobile nonholonomic robot, and general overview of educational mobile robots. In the second section, the following themes are covered: walking support robots, control system for wheelchairs, leg-wheel mechanism as a mobile platform, micro mobile robot for abdominal use, and the influence of the robot size in the psychological treatment. In the third section, there are chapters about I2C bus system, vertical displacement service robots, quadruped robots - kinematics and dynamics model and Epi.q (hybrid) robots. Finally, in the last section, the following topics are covered: skid-steered vehicles, robotic exploration (new place recognition), omnidirectional mobile robots, ball-wheel mobile robots, and planetary wheeled mobile robots.

INTECH
open science | open minds

InTech Europe
University Campus STeP Ri
Slavka Krautzeka 83/A
51000 Rijeka, Croatia
Phone: +385 (51) 770 447
Fax: +385 (51) 686 166
www.intechopen.com

InTech China
Unit 405, Office Block, Hotel Equatorial Shanghai
No.65, Yan An Road (West), Shanghai, 200040, China
中国上海市延安西路65号上海国际贵都大饭店办公楼405单元
Phone: +86-21-62489820
Fax: +86-21-62489821

IntechOpen